Half-life of the $I^\pi = 4^-$ intruder state in ^{34}P: $M2$ transition strengths approaching the island of inversion

P. J. R. Mason,[1] T. Alharbi,[1,2] P. H. Regan,[1] N. Mărginean,[3] Zs. Podolyàk,[1] E. C. Simpson,[1] N. Alkhomashi,[4] P. C. Bender,[5] M. Bowry,[1] M. Bostan,[6] D. Bucurescu,[3] A. M. Bruce,[7] G. Căta-Danil,[3] I. Căta-Danil,[3] R. Chakrabarti,[8] D. Deleanu,[3] P. Detistov,[9] M. N. Erduran,[10] D. Filipescu,[3] U. Garg,[11] T. Glodariu,[3] D. Ghiţă,[3] S. S. Ghugre,[8] A. Kusoglu,[6] R. Mărginean,[3] C. Mihai,[3] M. Nakhostin,[1] A. Negret,[3] S. Pascu,[3] C. Rodríguez Triguero,[7] T. Sava,[3] A. K. Sinha,[8] L. Stroe,[3] G. Suliman,[3] and N. V. Zamfir[3]

[1]*Department of Physics, University of Surrey, Guildford, Surrey GU2 7XH, United Kingdom*
[2]*Department of Physics, Almajmaah University, P.O. Box 66, 11952 Saudi Arabia*
[3]*Horia Hulubei National Institute of Physics and Nuclear Engineering (IFIN-HH), RO-077125 Bucharest, Romania*
[4]*KACST, P.O. Box 6086, Riyadh 11442, Saudi Arabia*
[5]*Department of Physics, Florida State University, Tallahassee, Florida, USA*
[6]*Department of Physics, Istanbul University, 34134 Istanbul, Turkey*
[7]*School of Computing, Engineering and Mathematics, University of Brighton, Brighton BN2 4GJ, United Kingdom*
[8]*UGC-DAE Consortium for Scientific Research, Kolkata Centre, Kolkata 700098, India*
[9]*Institute for Nuclear Research and Nuclear Energy (INRNE), Bulgarian Academy of Sciences, Sofia, Bulgaria*
[10]*Department of Computer Engineering, Istanbul Sabahattin Zaim University, Istanbul, Turkey*
[11]*Department of Physics, University of Notre Dame, Notre Dame, Indiana 46556, USA*

(Received 15 December 2011; revised manuscript received 22 May 2012; published 5 June 2012)

The half-life of the 2305-keV, $I^\pi = 4^{(-)}$ intruder state in ^{34}P has been measured as $t_{1/2} = 2.0(1)$ ns using γ-ray coincidence, fast-timing techniques with the Bucharest HPGe and $LaBr_3$:Ce detector array. Excited states in ^{34}P were populated using the ^{18}O(^{18}O, pn)^{34}P fusion-evaporation reaction at a beam energy of 36 MeV. Reduced transition probabilities have been calculated for different values of the $M2/E3$ mixing ratio, $\delta_{E3/M2}$, and compared with shell-model estimates. For small values of the mixing ratio, the $B(M2)$ value was found to be consistent with similar transitions associated with the occupation of neutron $f_{7/2}$ configurations in this mass region.

DOI: 10.1103/PhysRevC.85.064303 PACS number(s): 21.10.Tg, 23.20.Lv, 27.30.+t

I. INTRODUCTION

Far from the valley of stable atomic nuclei, deviations are observed from the conventional single-particle shell structure. Neutron-rich nuclei with $Z \sim 10$ and $N \sim 20$ are observed to have unexpectedly high binding energies, which has been linked to the onset of deformation [1]. This deformation is held to arise from the filling of the $f_{7/2}$ intruder orbital, which in stable nuclei lies above the $N = 20$ shell closure [2,3]. The size of the $N = 20$ shell gap is diminished for neutron-rich $Z \sim 10$ nuclei, allowing excitations from the $d_{3/2}$ to the $f_{7/2}$ orbital to become favored, leading to the region of anomalous shell structure known as the "island of inversion." The island of inversion is known to extend from neutron numbers $N =$ 20–22 for the Ne, Na, and Mg isotopes ($Z =$ 10–12) [3,4].

In the current work, we present spectroscopic results on electromagnetic transition rates in the $Z = 15$, $N = 19$ nucleus ^{34}P, which lies on the neutron-rich side of the valley of stability. The previously reported structure of ^{34}P includes a low-lying, yrast, $I = 4$ state at 2305 keV above the ground state. Several previous studies of this nucleus [5–8] have indicated a negative parity for this state, including a firm 4^- assignment by Bender *et al.* [8], though Krishichayan *et al.* [9] determined that the state has a 4^+ spin-parity. Limits on the half-life of the 2305-keV state have been set in the range of $300 \leqslant t_{1/2} \leqslant 2500$ ps [5]. The 1876-keV transition which depopulates this state has previously been assigned a mixed $M2$-$E3$ character by Chakrabarti *et al.* [6] with a mixing ratio in the range $-1.03 \leqslant \delta_{E3/M2} \leqslant -0.27$ deduced from polarization measurements. However, recent results by Bender *et al.* [10] give a value of $\delta_{E3/M2} = 0.0(1)$, indicating a pure $M2$ decay with no significant $E3$ component. The mixing ratio, $\delta_{E3/M2}$, of Bender *et al.* [10] was measured from the angular distribution of the 1876-keV transition by minimizing the χ^2 value of the fitted distribution as a function of δ for given initial and final spins [10].

Ollier *et al.* [7] suggested that the 2305-keV state had a spin-parity of 4^- and it was based predominantly on a $\pi s_{1/2} \otimes \nu f_{7/2}$ configuration, with the 2^+ state to which it decays having a $\pi s_{1/2} \otimes \nu d_{3/2}^{-1}$ character. Thus, the transition between these states would be expected to proceed via a $\nu f_{7/2} \rightarrow \nu d_{3/2}$ single-particle $M2$ transition. Shell-model calculations by Bender *et al.* [8] agreed with the prediction of a predominant $\pi s_{1/2} \otimes \nu d_{3/2}^{-1}$ configuration for the 2^+ state with small contributions from the $\pi d_{3/2}$ orbital. The calculations also predicted dominance of the $\pi s_{1/2} \otimes \nu f_{7/2}$ configuration for the 4^- state, with contributions from the $\nu s_{1/2}$, $\nu d_{5/2}$, and $\pi d_{3/2}$ orbitals. These admixtures of other orbitals in the single-particle configurations allow for a mixed $M2$-$E3$ transition between the states.

Assignment of a negative parity to the 2305-keV state in ^{34}P provides a smooth continuation in the systematic lowering of the energies of the 4^- states through the phosphorus isotopic chain (see Fig. 18 of Ref. [11]). The same trend in 4^- energy

with increasing neutron number is observed in the $Z = 13$ aluminum isotopes [11]. Intruder states in nuclei in the *sd* shell necessarily involve promotion of a nucleon above the $N = 20$ shell closure into the *fp* shell. Thus the lowering of the energies of intruder states as a function of increasing neutron number in *sd* shell nuclei demonstrates the weakening of the $N = 20$ shell gap for nuclei as one moves from the region of stable isotopes toward the island of inversion. The $\nu d_{3/2} \rightarrow \nu f_{7/2}$ excitation thought to be responsible for 4^- states in phosphorus and aluminum isotopes is the same excitation thought to be responsible for the ground-state configurations in island of inversion nuclei. Understanding the nature of configurations involving intruder orbitals in this region is important in describing the evolution from the normal shell structure toward the deformed ground-state configurations in the island of inversion.

The half-life of the 2305-keV state has been measured in this work using a fast-timing techniques with the aim of determining reduced transition probabilities for the depopulating 1876-keV γ ray with the mixing ratios measured in previous studies [6,10]. The precision measurement of the half-life in the present work is reported with much improved accuracy compared to the limits set by Asai *et al.* [5]. The effect of the measured half-life on the interpretation of the parity of the state is discussed.

II. EXPERIMENT AND DATA ANALYSIS

Excited states in ^{34}P were populated following the ^{18}O(^{18}O, pn)^{34}P reaction at a beam energy of 36 MeV. The beam was provided by the Tandem van de Graaff accelerator at the National Institute of Physics and Nuclear Engineering, Bucharest. The Ta_2O_5 target was prepared by heating a 50 mg/cm^2 Ta foil in an atmosphere of enriched oxygen and the equivalent thickness of ^{18}O was estimated to be 1.6 mg/cm^2 on both faces of the target [6]. The experiment ran for a total of 156 h during which the average beam intensity was $\sim$20 particle·nA.

Gamma rays produced in the reaction were detected by an array of eight HPGe detectors and seven $LaBr_3$:Ce detectors placed around the target chamber. Of the seven $LaBr_3$:Ce detectors in the array, three had $2'' \times 2''$ cylindrical crystals, two had $1.5'' \times 1.5''$ cylindrical crystals, and two had $1'' \times 1.5''$ conical crystals [12]. Timing information for each $LaBr_3$:Ce detector was recorded with a time-to-amplitude converter (TAC), with the start signal taken from the $LaBr_3$:Ce detector and a stop signal from the master trigger distributed to all the TAC units as described in Ref. [12]. By using this method, the absolute time difference between any two $LaBr_3$:Ce detectors is extracted by subtracting their time differences relative to the trigger. For this experiment, the master trigger condition was the detection of either three coincident HPGe signals or two coincident $LaBr_3$:Ce signals. A total of $\sim 10^9$ $LaBr_3$:Ce coincidences were detected during the experiment.

The array contained eight unsuppressed HPGe detectors, each with a relative efficiency of $\sim$50% [12]. Five of the HPGe detectors were placed at 143°, two at 90°, and one at 30° with respect to the beam direction. The HPGe detectors can be used in such fast-timing experiments to set coincidence gates to select a particular γ-ray cascade of interest to create clean spectra from which time differences are to be measured in the $LaBr_3$:Ce detectors [12]. However, in the present experiment, to increase the statistics in the time-difference spectra, the HPGe detectors were not used for this purpose. In this experiment it was possible to measure the time differences of interest from the $LaBr_3$:Ce detectors without requiring a gate in the HPGe detectors.

Calibration of the HPGe and $LaBr_3$:Ce detectors in energy and relative efficiency was performed using ^{56}Co, ^{60}Co, and ^{152}Eu sources placed at the target position. To account for the instability in the energy response of the $LaBr_3$:Ce detectors, a run-by-run gain-matching procedure was also applied. Time walk correction for the $LaBr_3$:Ce detectors was performed with ^{56}Co and ^{60}Co sources using the method described in Ref. [12], in which the energy dependence of the time walk for each detector is fitted with a polynomial function and corrected in off-line analysis.

Data were sorted off-line into a series of two- and three-dimensional histograms (matrices and cubes) and analyzed with the GASPWARE [13] software suite. Of central importance are $LaBr_3$:Ce $E_{\gamma 1}$-$E_{\gamma 2}$-ΔT cubes, described in Ref. [12], which allow gates to be set on two γ-ray energies in the $LaBr_3$:Ce detectors and the associated time-difference spectrum to be extracted.

III. RESULTS

Figure 1 shows the partial level scheme for ^{34}P relevant to this work. The half-life of the 2305-keV state was determined from the time difference between the 1048- and 429-keV transitions. Ideally, the half-life is measured by taking the time

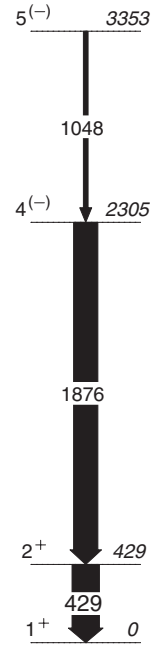

FIG. 1. Partial level scheme for ^{34}P relevant to this work, adapted from Refs. [6,8].

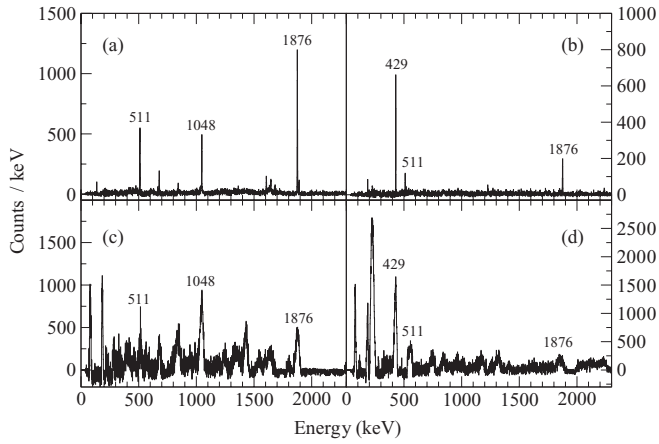

FIG. 2. Coincidence γ-ray spectra created from γ-γ matrices in this work. The top panels show spectra from the HPGe detectors when gating on transitions detected in the HPGe detectors. The bottom panels show the equivalent spectra from the $LaBr_3$:Ce detectors when gating on transitions detected in the $LaBr_3$:Ce detectors. Panels (a) and (c) show γ-ray spectra in coincidence with the 429-keV transition in ^{34}P. Panels (b) and (d) show spectra in coincidence with the 1048-keV transition in ^{34}P.

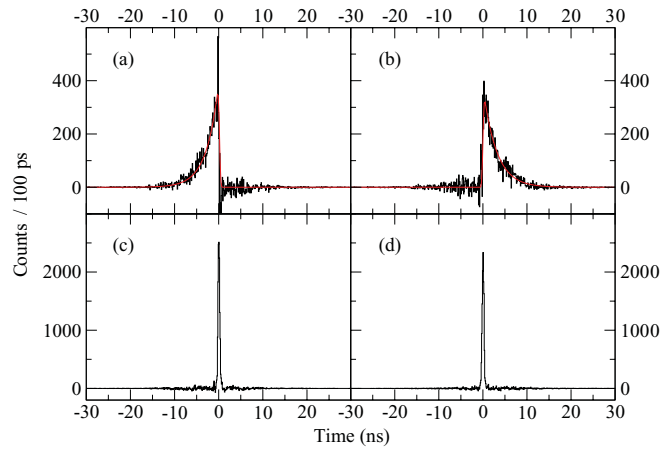

FIG. 3. (Color online) Time spectra for ^{34}P from the $LaBr_3$:Ce $E_{\gamma 1}$-$E_{\gamma 2}$-ΔT cube, showing the time difference between (a) 429- and 1048-keV γ rays, (b) 1048- and 429-keV γ rays, (c) 429- and 1876-keV γ rays, and (d) 1876- and 429-keV γ rays. The solid lines in panels (a) and (b) are Gaussian-exponential convolution fits to the spectra.

difference for transitions directly feeding and depopulating the level of interest. However, the $LaBr_3$:Ce efficiency for the 1876-keV γ ray depopulating the 2305-keV state was not sufficient in the current work, so the time difference was taken between the 1048- and 429-keV transitions to maximize statistics. Although, the measured 1048–429-keV time-difference spectrum will depend on the half-lives of both the 2305-keV and 429-keV states (see Fig. 1), the half-life of the 429-keV state was limited in Ref. [8] to $t_{1/2} < 1$ ps, which is negligible compared to the expected half-life of the 2305-keV state of $300 \leqslant t_{1/2} \leqslant 2500$ ps [5] and too short to be measured with direct electronic timing methods. Thus the 1048–429-keV time difference has been assumed to be solely representative of the decay of the 2305-keV state.

Figure 2 shows sample γ-ray energy spectra created from a HPGe-HPGe coincidence matrix and equivalent spectra from a $LaBr_3$:Ce-$LaBr_3$:Ce coincidence matrix in this work. The spectra from the $LaBr_3$:Ce-$LaBr_3$:Ce matrix show significant contamination from other nuclei populated in the reaction. This contamination is present because the energy resolution of the $LaBr_3$:Ce detectors is not sufficient to separate two (or more) closely spaced photopeaks in the spectra and so coincidence gates placed on those spectra may contain the tails of photopeaks with similar energy from other nuclei. However, it can be seen that these spectra are clean in the region of the 1048- and 429-keV peaks from ^{34}P. Thus it is possible to create clean 1048–429-keV time-difference spectra for ^{34}P from the $LaBr_3$:Ce $E_{\gamma 1}$-$E_{\gamma 2}$-ΔT cube.

Figure 3 shows $LaBr_3$:Ce time-difference spectra created in the present work. Panels (a) and (b) show the time difference between the 1048- and 429-keV transitions of ^{34}P, with the "reversed" spectrum in panel (a) the result of starting the time difference with the depopulating 429-keV transition and stopping with the feeding 1048-keV. Panels (c) and (d) show the time difference between the 1876- and 429-keV transitions, again with panel (c) showing the "reversed" gate order. The 1876–429-keV time difference for the half-life of the yrast 2^+ state in ^{34}P displayed no measurable shift between the centroids of these spectra, in agreement with the half-life limits in Ref. [8]. Gaussian fits to the 1876–429-keV time-difference spectra give a prompt $LaBr_3$:Ce time resolution (full width at half maximum, FWHM) for the full array of 470(10) ps.

The 1048–429-keV time-difference spectra were fitted with an exponential decay convoluted with a Gaussian time resolution. The FWHM of the Gaussian and $\Delta T = 0$ position were fixed from fits to the 1876–429-keV time-difference spectra. These fits gave the half-life of the 2305-keV state in ^{34}P to be $t_{1/2} = 2.0(1)$ ns. This result is consistent with the previously reported limits of $300 \leqslant t_{1/2} \leqslant 2500$ ps [5].

IV. DISCUSSION

Experimental reduced transition probabilities, $B(M2)$ and $B(E3)$, for the 1876-keV transition are obtained using the relations

$$B(M2) = \frac{5.12 \times 10^{-8}}{t_{1/2} E_\gamma^5} \frac{1}{\left(1 + \delta^2_{E3/M2}\right)} \mu_N^2 \text{ fm}^2 \qquad (1)$$

and

$$B(E3) = \frac{1.21 \times 10^{-3}}{t_{1/2} E_\gamma^7} \frac{\delta^2_{E3/M2}}{\left(1 + \delta^2_{E3/M2}\right)} e^2 \text{ fm}^6, \qquad (2)$$

where E_γ is the γ-ray energy (in MeV), $t_{1/2}$ is the half-life of the state (in seconds), and μ_N is the nuclear magneton. Weisskopf single-particle estimates for the reduced transition probabilities are given by

$$B_W(M2) = 1.65 A^{2/3} \mu_N^2 \text{ fm}^2 \qquad (3)$$

and

$$B_W(E3) = 5.94 \times 10^{-2} A^2 e^2 \text{ fm}^6, \qquad (4)$$

TABLE I. Reduced transition probabilities for the 1876-keV γ ray in ^{34}P at values of the mixing ratio, $\delta_{E3/M2}$, taken from Refs. [6] and [10].

$t_{1/2}$ (ns)	$\delta_{E3/M2}$	$B(M2)$		$B(E3)$	
		(μ_N^2 fm^2)	(W.u.)	(e^2 fm^6)	(W.u.)
2.0(1)	0.0(1) [10]	1.10(6)	0.064(3)	0	0
2.0(1)	-0.27[a] [6]	1.03(5)	0.059(3)	505(25)	7.35(38)
2.0(1)	-1.03[b] [6]	0.534(26)	0.031(2)	3820(190)	55.7(28)

[a]Upper limit [6].
[b]Lower limit [6].

where A is the mass number. Table I gives the experimental reduced transition probabilities for the 1876-keV γ ray in ^{34}P computed for values of the mixing ratio, $\delta_{E3/M2}$, reported in Refs. [6,10]. Figure 4 shows the $B(M2)$ and $B(E3)$ values as a function of $\delta_{E3/M2}$ over the full range of possible values.

The 2305-keV state was assigned to have a 4^+ spin-parity by Krishichayan *et al.* [9] based on γ-ray polarization measurements, which suggested an $E2$ character for the 1876-keV transition. This polarization was measured from the asymmetry of Compton scattering in clover detectors. The asymmetry parameter, Δ_{IPDCO}, was reported with a large error for the 1876-keV transition with a value of $\Delta_{\mathrm{IPDCO}} = 0.15(17)$ [9]. The 4^+ assignment was ruled out by Chakrabarti *et al.* [6] as their measured limits for the mixing ratio implied an unacceptably large $M3$ strength. Taking the recent result by Bender *et al.* [10] of $\delta = 0.0(1)$ with a 4^+ spin-parity for the 2305-keV state would preclude any significant $M3$ component [i.e., $\delta_{M3/E2} = 0.0(1)$]. By using $\delta_{M3/E2} = 0.0(1)$, the argument made by Chakrabarti *et al.* [6] based on the unacceptably large $M3$ component is no longer applicable, potentially allowing for the assignment of a 4^+ spin-parity for the 2305-keV state. The half-life measured in the present work would correspond to the upper limit of $B(E2) = 0.0122(6)$ e^2 fm^4 or $B(E2) = 0.0019(1)$ W.u., which is several orders of magnitude smaller than that which might be expected from a 4^+ state of this type (see the shell-model calculations below).

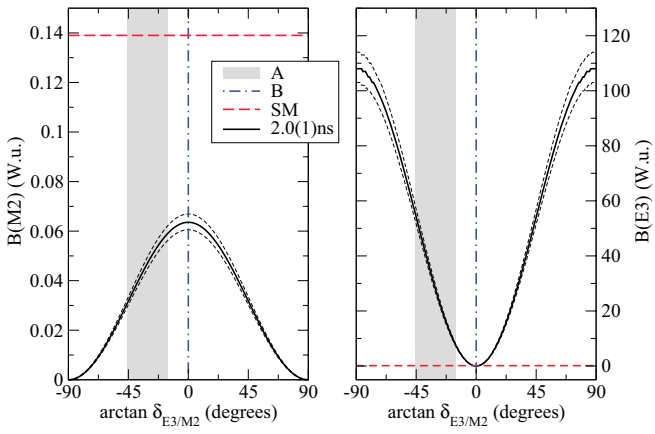

FIG. 4. (Color online) $B(M2)$ (left) and $B(E3)$ (right) values for the $4^- \rightarrow 2^+$ transition in ^{34}P as a function of the mixing ratio, $\delta_{E3/M2}$, calculated with $t_{1/2} = 2.0(1)$ ns. The curving dashed lines represent the limits defined by the error in the half-life measurement. The shaded regions (A) represent the limits of $-1.03 \leqslant \delta_{E3/M2} \leqslant -0.27$ from Ref. [6] and the vertical dash-dotted lines (B) are the measurement of $\delta_{E3/M2} = 0.0(1)$ from Ref. [10]. The horizontal dashed lines are the theoretical shell-model (SM) estimates of $B(M2)$ and $B(E3)$ from this work.

Conversely, assigning a 4^- spin-parity for the 2035-keV state and an $M2$ character with $\delta_{E3/M2} = 0$ for the 1876-keV transition gives an experimental $B(M2) = 0.064(3)$ W.u. This falls within the range of other reported $\nu f_{7/2} \rightarrow \nu d_{3/2}$ $M2$ transitions in this mass region [14], ranging from 0.0330(10) W.u. in ^{47}Sc [15] to 0.63(6) W.u. in ^{37}Cl [16]. Notably, the result is similar to the $M2$ strengths from intruder states in neighboring $N = 19$ nuclei, ^{33}Si [17], ^{35}S, ^{36}Cl, and ^{37}Ar [16], shown in Fig. 5. Also shown in Fig. 5 are the mixing ratios for the $N = 19$ nuclei.

Due to the similarity with reduced transition probabilities in nearby nuclei, along with the arguments set out by Bender *et al.* [8] and Ollier *et al.* [7], we prefer the assignment of a pure $M2$ or mixed $M2$-$E3$ character for the 1876-keV transition and thus a 4^- spin-parity for the 2305-keV state. The reason for the incompatibility between the experimental mixing ratios in Refs. [6,10] is unclear, but a mixing ratio of $\delta_{E3/M2} = 0$ [10] or a value close to the upper limit of $\delta_{E3/M2} = -0.27$ both give $B(M2)$ values that follow the trend of reduced transition probabilities for the neighboring isotones. A mixing ratio close to the lower limit of $\delta_{E3/M2} = -1.03$ in Ref. [6] gives a $B(M2)$ that is smaller than those of the neighboring isotones and does not follow the apparent systematic trend (see Fig. 5). While an $E2$ character for the 1876-keV transition cannot be ruled out unambiguously in the present work, we conclude that a 4^- spin-parity is by far the more probable assignment for the 2305-keV state based on the transition strength arguments as allowed by the current measurement.

Assignment of a negative parity for the 2305-keV state shows the presence of low-lying configurations based on intruder orbitals in ^{34}P. These configurations necessarily involve the promotion of a nucleon above the $N = 20$ shell closure and demonstrate the weakening of this closure approaching the island of inversion. The similarity to other transitions in this region suggests that the transition largely comprises the $\nu f_{7/2} \rightarrow \nu d_{3/2}$ $M2$ single-particle transition. This is analogous to the excitations from the $d_{3/2}$ to the $f_{7/2}$ orbital deemed to be responsible for the ground-state configurations in island of inversion nuclei [2].

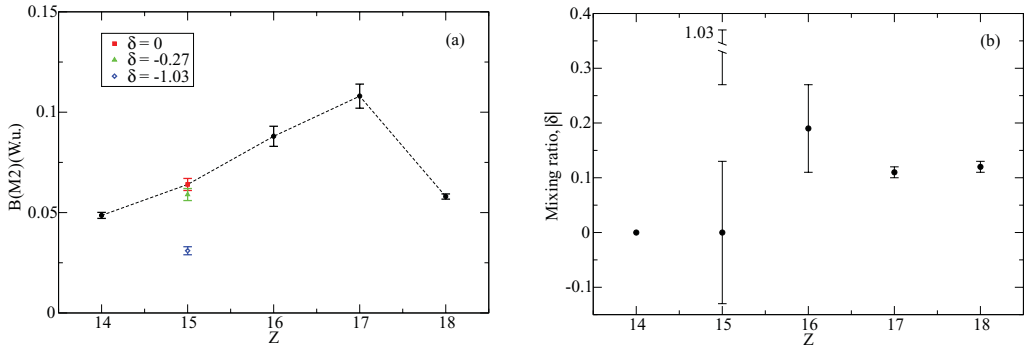

FIG. 5. (Color online) (a) Systematics of experimental $B(M2)$ values and (b) experimental mixing ratios, $|\delta|$, for $N = 19$ isotones. Values for ^{34}P are shown at mixing ratios of $\delta_{E3/M2} = 0.0(1)$ [10] and the upper and lower limits of $\delta_{E3/M2} = -0.27$ and $\delta_{E3/M2} = -1.03$ from Ref. [6].

Shell-model calculations were performed for this work with the OXBASH code [18] using the WBP interaction [19] modified by lowering the single-particle energies of the $f_{7/2}$ and $p_{3/2}$ orbitals by 1.8 and 0.5 MeV, respectively. This modification was made in the work by Bender *et al.* [8], who termed the modified interaction WBP-a, to better reproduce the energies of the negative-parity states in ^{32}P. As in Ref. [8], the model space included unrestricted occupation of orbitals in the *sd* shell, with a closed ^{16}O core, and 0 or 1 particles shared between the $f_{7/2}$ or $p_{3/2}$ orbitals.

Theoretical $B(M2)$ and $B(E3)$ values for the 1876-keV transition were extracted from the above shell-model calculations. The standard effective charges of $1.5e$ and $0.5e$ for protons and neutrons, respectively, were used in calculating electric transitions and the free nucleon g factors were used for magnetic transitions. Values of $B(M2) = 0.139$ W.u. and $B(E3) = 0.127$ W.u. and $\delta_{E3/M2} = -0.023$ were obtained. The disparity between the present theoretical $B(M2)$ and the value of $B(M2) = 0.19$ W.u. obtained by Bender *et al.* [8] with the same interaction is due to differences in the choice of harmonic oscillator scaling factor for the transition rate, which relates to the size of the nuclear charge radius. In the present calculations $b = 1.88$ fm is used for the size parameter of the harmonic oscillator wave function, whereas $b = 1$ fm was used by Bender *et al.* and then scaled by a factor of $1.2A^{1/3}$. The shell-model estimates of $B(M2)$ and $B(E3)$ are shown along with the range of experimental values in Fig. 4.

The mixing ratio of $\delta_{E3/M2} = -0.023$ predicted by the shell model indicates an almost pure $M2$ character for the 1876-keV transition. This is in agreement with the value $\delta_{E3/M2} = 0.0(1)$ found by Bender *et al.* [10], but it disagrees with the stronger $E3$ component reported by Chakrabarti *et al.* [6]. The shell model overestimates $B(M2)$ for all values of $\delta_{E3/M2}$, being more than a factor of 2 greater than the experimental $B(M2)$ calculated with $\delta_{E3/M2} = 0$.

The yrast 4^+ state predicted by the shell-model calculations was at an excitation energy of 3788 keV above the ground state. Theoretical transition rates from the this state to the lowest 2^+ state were calculated to be $B(E2) = 14.0$ W.u. and $B(M3) = 6.29$ W.u., with a mixing ratio of $\delta_{M3/E2} = -0.043$. From the half-life of the 2305-keV state, the experimental upper limit on $B(E2)$ for the 1876-keV transition is $B(E2) = 0.0019(1)$ W.u. which is almost four orders of magnitude smaller than the shell-model prediction. Barring any special structural effects for the 2305-keV state, it is unlikely that $B(E2)$ would be so much smaller than the shell-model estimate for the 4^+ state. Without an explanation for the large additional hindrance necessary to produce the experimentally observed half-life, a 4^+ spin-parity assignment for the 2305-keV state is extremely unlikely, supporting the negative-parity assignment for this state.

Theoretical calculations of $B(M2)$ and $B(E3)$ values for the 1876-keV transition were also made using the unmodified WBP interaction [19], which gave values of $B(M2) = 0.053$ W.u. and $B(E3) = 0.009$ W.u. The difference in the reduced transition probabilities calculated with the WBP and WBP-a interactions is due to the different admixtures of orbitals in the state configurations. The 4^- state calculated with the WBP interaction contains a significantly larger admixture of the $p_{3/2}$ state compared to the WBP-a calculation. Although the WBP interaction predicts a $B(M2)$ value within the range of the possible experimental values, it greatly overestimates the excitation energy of the 4^- state and other negative-parity states as described in Ref. [8]. It is not expected that shell-model calculations of the type presented in the work will give very accurate reduced transition probabilities for cross-shell transitions and it is unlikely that further tuning of the single-particle energies or model space will yield any additional physical insight into the 2305-keV state in ^{34}P.

V. SUMMARY

The half-life of the 2305-keV state in ^{34}P has been measured in this work to be $t_{1/2} = 2.0(1)$ ns. By assuming $I^\pi = 4^-$, $B(M2)$ and $B(E3)$ reduced transition probabilities have been obtained for different values of the mixing ratio, $\delta_{E3/M2}$. For small values of the mixing ratio, $B(M2)$ follows the systematics of other decays identified as $\nu f_{7/2} \rightarrow \nu d_{3/2}$ transitions in this mass region [14]. Due to the similarity of the reduced transition probability to other transitions in the region, it is likely that the 1876-keV transition largely comprises a $\nu f_{7/2} \rightarrow \nu d_{3/2}$ single-particle transition. This supports the negative-parity assignment and a predominantly $\pi s_{1/2} \otimes \nu f_{7/2}$ configuration for the 2305-keV state as reported by other authors [5–8] over the $I^\pi = 4^+$ assignment of Krishichayan

et al. [9]. A negative-parity assignment for this state indicates the involvement of intruder orbitals above the $N = 20$ shell closure and demonstrates the weakening of the shell gap approaching the island of inversion.

Shell-model calculations performed in this work predict an almost pure $M2$ character for the 1876-keV γ ray with $\delta_{E3/M2} = -0.023$. These calculations give a value of $B(M2) = 0.139$ W.u. for a transition between the yrast 4^- and 2^+ states, which is within the same order of magnitude as the experimental limits of the $B(M2)$ value. The shell-model estimate for the $B(E2)$ value from the lowest 4^+ state is $B(E2) = 14.0$ W.u. which is almost four orders of magnitude larger than the experimental upper limit of $B(E2) = 0.0019(1)$ W.u. for the 1876-keV transition. The unexpectedly large hindrance required to make a positive-parity assignment for the 2305-keV state also supports the negative-parity assignment for this state.

ACKNOWLEDGMENTS

We would like to thank the staff of the Horia Hulubei National Institute of Physics and Nuclear Engineering (IFIN-HH), Romania, for their support during this experiment and John Greene from Argonne National Laboratory for preparing the target. This work was supported by the Science and Technology Facilities Council (STFC) (UK), the Romanian Ministry for Education and Research [Contracts Module3-24EU-ISOLDE and PN-II-ID-PCE-2011-3-0367(UEFISCDI)], ANCS (Romania), the Scientific and Technological Research Council of Turkey (TÜBİTAK) under the International Bilateral Cooperation Project No. 109T613, and the US National Science Foundation (Grants No. PHY07-58100, No. PHY-1068192, and No. PHY-07-56474). TA acknowledges the support of Almajmaah University, Saudi Arabia.

[1] C. Thibault *et al*., Phys. Rev. C **12**, 644 (1975).
[2] B. H. Wildenthal and W. Chung, Phys. Rev. C **22**, 2260 (1980).
[3] E. K. Warburton, J. A. Becker, and B. A. Brown, Phys. Rev. C **41**, 1147 (1990).
[4] N. A. Orr *et al*., Phys. Lett. B **258**, 29 (1991).
[5] M. Asai, T. Ishii, A. Makishima, M. Ogawa, and M. Matsuda, in *Proceedings of the Third International Conference on Fission and Properties of Neutron-Rich Nuclei*, edited by J. H. Hamilton, A. V. Ramayya, and H. K. Carter (World Scientific, Singapore, 2002), pp. 295–297.
[6] R. Chakrabarti *et al*., Phys. Rev. C **80**, 034326 (2009).
[7] J. Ollier *et al*., Phys. Rev. C **71**, 034316 (2005).
[8] P. C. Bender *et al*., Phys. Rev. C **80**, 014302 (2009).
[9] Krishichayan *et al*., Eur. Phys. J. A **29**, 151 (2006).
[10] P. C. Bender *et al*., Phys. Rev. C **85**, 044305 (2012).
[11] T. A. Hinners *et al*., Phys. Rev. C **77**, 034305 (2008).
[12] N. Mărginean *et al*., Eur. Phys. J. A **46**, 329 (2010).
[13] D. Bazzacco and N. Mărginean (private communication).
[14] J. Keinonen *et al*., Phys. Rev. C **14**, 160 (1976).
[15] T. W. Burrows, Nucl. Data Sheets **108**, 923 (2007).
[16] P. M. Endt and R. B. Firestone, Nucl. Phys. A **633**, 1 (1998).
[17] J. Chen and B. Singh, Nucl. Data Sheets **112**, 1393 (2011).
[18] B. A. Brown, A. Etchegoyen, N. S. Godwin, W. D. M. Rae, W. A. Richter, W. E. Ormand, E. K. Warburton, J. S. Winfield, L. Zhao, and C. H. Zimmerman, MSU-NSCL Report No. 1289.
[19] E. K. Warburton and B. A. Brown, Phys. Rev. C **46**, 923 (1992).